APPLIED PHYSICS LETTERS VOLUME 83, NUMBER 17 27 OCTOBER 2003

Selective formation of ZnO nanodots on nanopatterned substrates by metalorganic chemical vapor deposition

Sang-Woo Kim,[a] Teruhisa Kotani, and Masaya Ueda
Department of Electronic Science and Engineering, Kyoto University, Yoshida-honmachi, Sakyo, Kyoto 606-8501, Japan

Shizuo Fujita
International Innovation Center, Kyoto University, Yoshida-honmachi, Sakyo, Kyoto 606-8501, Japan

Shigeo Fujita
Department of Electronic Science and Engineering, Kyoto University, Yoshida-honmachi, Sakyo, Kyoto 606-8501, Japan

(Received 31 March 2003; accepted 3 September 2003)

Selective formation of ZnO nanodots was accomplished by metalorganic chemical vapor deposition on nanopatterned SiO_2/Si substrates. Self-organized ZnO nanodots were selectively formed in nanopatterned lines of Si created by etching of SiO_2 with focused ion beam (FIB), whereas any nanodots were hardly observed on the SiO_2 surface in the vicinity of the FIB-sputtered Si areas. The mechanism of the selective formation of ZnO nanodots on FIB-nanopatterned lines is mainly attributed to the effective migration of Zn adatoms diffusing on the SiO_2 surface into the Si lines followed by the nucleation at surface atomic steps and kinks created by Ga^+ ion sputtering. Cathodoluminescence measurements confirmed that the emission originated from the selectively grown ZnO nanodots. *© 2003 American Institute of Physics.* [DOI: 10.1063/1.1622795]

Nanoscale semiconductor structures such as quantum wells, wires, and dots have stimulated great interest due to the predicted improvement in device performance.[1] Many unique and fascinating properties have been demonstrated in semiconductor nanostructures.[2–4] ZnO is of interest for electrical and optical devices with its multifunctionality as well as excitonic effects.[5] In these regards, the realization of low-dimensional ZnO nanostuctures is strongly demanded, resulting in a lot of nanoscale, nanophotonic, and nanomagnetic devices. Even though the realization of self-assembled low-dimensional ZnO nanostructures such as nanowires[6] and quantum dots[7] has been reported, the ZnO nanostructures grown on substrates are randomly distributed with fluctuations on their size and their position. One of the major bottlenecks of the nanoscale devices relies on the lack of reproducibility of naturally formed nanostructures, which indicates that a better control of the periodicity, shape, and size of nanostructures should be developed in order to realize nanoscale multifunctional devices.

Focused ion beam (FIB) has been regarded as an important tool for maskless patterning, which is the outstanding capability of FIB compared with other lithographic techniques.[8,9] In this letter, we report the selective formation of ZnO nanodots on FIB-nanopatterned SiO_2/Si substrates by metalorganic chemical vapor deposition (MOCVD).

The SiO_2 layer with a thickness of 50 nm was thermally formed in a furnace in oxygen atmosphere at 1100 °C. The SiO_2/Si samples were immediately transferred into the FIB chamber (SEIKO SMI-2050). Nanopatterned lines in 8×8 μm^2 fields were patterned by FIB on SiO_2 (50 nm)/Si (111) substrates using 30 keV Ga^+ ions at a beam current of 48 pA with an ion dose of 3.4×10^{17} cm^{-2} as shown in Fig. 1(a). The estimated diameter of the beam was 23 nm.

An atomic force microscope (AFM), (SEIKO SPA-400) image of the lines patterned by FIB is shown in Fig. 1(b) together with the cross-sectional image [Fig. 1(c)] obtained by a line scan of the AFM profile. The SiO_2 layer (50 nm) on Si (111) was successfully removed by the energetic Ga^+ ion sputtering. The etched depth of SiO_2/Si substrates was about 100 nm. The width of individual nanopatterned lines was 390 nm at the SiO_2 surface.

The ZnO nanodots on nanopatterned SiO_2/Si (111) sub-

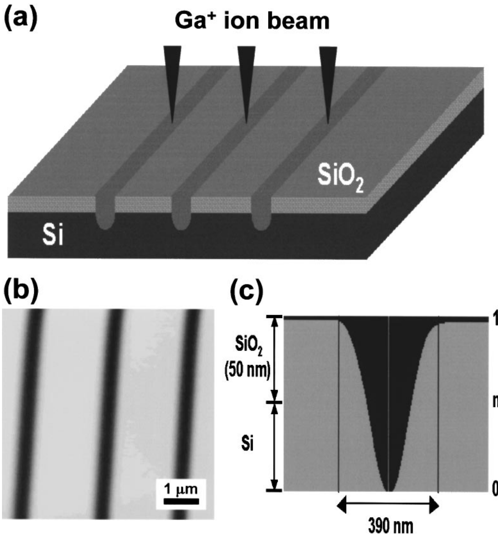

FIG. 1. (a) A schematic image of FIB-nanopatterning of a SiO_2/Si substrate with 30 keV Ga^+ ions at a beam current of 48 pA. The beam diameter was 23 nm. (b) An AFM image of FIB-nanopatterned lines. (c) A cross-section image of a single nanopatterned line, which was obtained by a line scan of the AFM profile.

---

[a] Electronic mail: swkim@fujita.kuee.kyoto-u.ac.jp

0003-6951/2003/83(17)/3593/3/$20.00

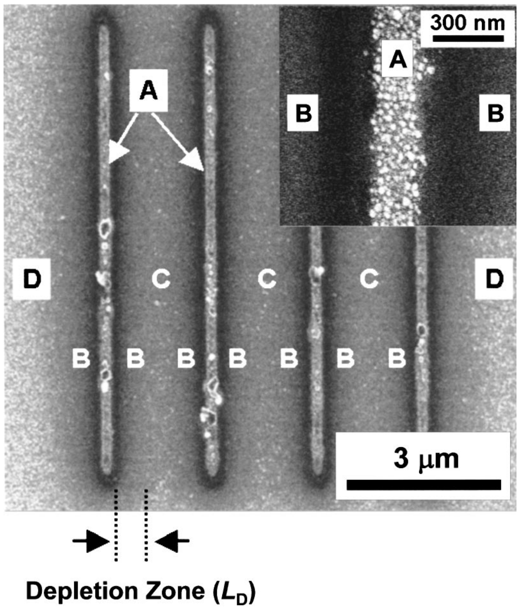

FIG. 2. Typical FE–SEM images of ZnO nanodots grown in the nanopatterned lines with an interdistance of 2 μm at 550 °C with the DEZn flow rate of 3 μmol/min. The selective formation of ZnO nanodots is clearly shown in FIB-sputtered Si areas (A). On the other hand, ZnO nanodots are hardly observed in depletion zones (B). Several ZnO nanodots, which could not diffuse from the SiO_2 surface to nanopatterned Si areas, in middle areas between nanolines is observed (C). ZnO nanodots form densely on the planar SiO_2 surface outside the ion implanted areas (D). Inset is a magnified FE–SEM image of the selectively formed ZnO nanodots with the average diameter of about 15 nm in the FIB-sputtered Si area (A).

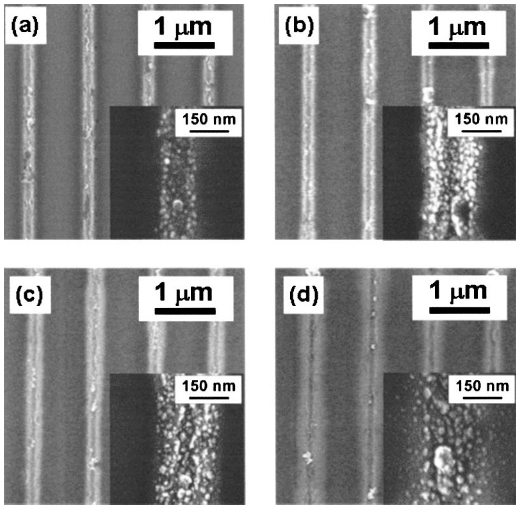

FIG. 3. Plan-view FE–SEM images of selectively grown ZnO nanodots by the DEZn flow rate of 1 μmol/min at different growth temperature in FIB-nanopatterned lines with an interdistance of 1 μm. Insets show ZnO nanodots in a single FIB-nanopatterned line. (a) 500, (b) 550, (c) 600, and (d) 650 °C.

strates were grown by MOCVD using nitrous oxide (N_2O) gas as an oxygen source and diethylzinc (DEZn) as a zinc source at different temperatures with intervals of 50 °C in the range of 500–650 °C for 22 s. Typical flow rate of DEZn was 1 or 3 μmol/min with that of N_2O 7000 μmol/min, and the total pressure of the reactor was fixed at 200 Torr. The grown patterns of ZnO nanodots were investigated by a field-effect scanning electron microscope (FE–SEM) (HITACHI S-4500). The optical property of selectively grown ZnO nanodots was characterized by cathodoluminescence (CL) (JEOL JSM-6500F) measurements at RT.

Figure 2 shows FE–SEM images of ZnO nanodots grown at 550 °C with the DEZn flow rate of 3 μmol/min on the SiO_2/Si substrate where the interdistance of nanopatterns is 2 μm. The magnified image shown as the inset of Fig. 2 clearly identifies the selective formation of ZnO nanodots with the average diameter of about 15 nm in the FIB-sputtered Si area (A). ZnO nanodots are hardly observed on the SiO_2 layer in the close vicinity of the FIB-sputtered Si areas (B). Several ZnO nanodots are seen in middle areas between the nanolines (C). On the other hand, ZnO nanodots form densely on the planar SiO_2 surface (D) outside the ion-implanted areas.[10,11] The existence of a so-called ‘‘depletion zone’’ (B), where the nanodots cannot be seen, indicates that Zn adatoms on SiO_2 diffuse to the nanopatterned Si areas and preferably form nanodots in the nanopatterned Si area rather than on the SiO_2 mask region.

In general, the surface diffusivity of metal adatoms on SiO_2 is much larger than that on Si, which is attributed to the low sticking coefficient of metal adatoms on a SiO_2 surface.[12,13] This fact can suggest that the surface diffusion length of a Zn adatom for successive reactions to make ZnO is different on SiO_2 and Si. Zn adatoms have a higher surface mobility and a shorter surface lifetime on the SiO_2 than on the Si surface, resulting in preferred migration of adsorbed Zn atoms from the SiO_2 to the Si surface with stable bonding configurations. In addition, the selective formation of ZnO nanodots in nanopatterned lines can be quite associated with the generation of surface atomic steps created by Ga^+ ion sputtering. Surface atomic step generated by sputtering has been shown to strongly increase the growth rate of InP on FIB-patterned GaAs,[14] which suggests that introducing surface steps and kinks enhances the nucleation probability of depositing material. The nucleation on the steps and kinks in the sputtered areas acts as a sink for migrating surface adatoms and consumes adsorbed species transported by surface diffusion. Namely, Zn adatoms near the patterned boundary during the growth of ZnO can easily migrate from SiO_2 to Si and form stable nucleation on Si, resulting in the selective formation of ZnO nanodots on nanopatterned Si.

The depletion zone width (L_D) was found to be below about 0.5, 0.8, and 0.9 μm at the growth temperature of 500, 550, and 600 °C, respectively. As mentioned before, the existence of the depletion zone indicates that Zn atoms prefer to form ZnO dots on the patterned area rather than on the SiO_2 surface. L_D gives key information for the design of periodic nanopatterned lines for selective growth because random ZnO dots on SiO_2 cannot be formed when the distance between the nanopatterns is smaller than $2L_D$. The maximum lengths of 1 (500 °C), 1.6 (550 °C), and 1.8 μm (600 °C) for the diffusion of Zn adatoms from the SiO_2 surface to the nanopatterned Si area under the DEZn flow rate of 3 μmol/min are smaller than the interdistance of 2 μm between the nanopatterned lines. This fact explains why the several ZnO nanodots remain in the areas (C) in Fig. 2. In fact, the selective formation of ZnO nanodots was achieved without any depletion regions when the nanopatterns with narrower interdistance and the growth condition with the low DEZn flow rate were applied, as will be shown in Fig. 3.

FE–SEM images of the ZnO nanodots selectively grown

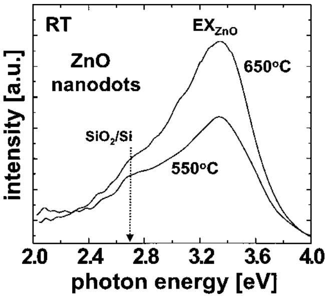

FIG. 4. CL spectra from ZnO nanodots shown in Figs. 3(b) and 3(d), measured at RT.

on the FIB-nanopatterned SiO_2/Si substrates with an interdistance of 1 μm at different growth temperatures from 500 to 650 °C are presented in Fig. 3. The flow rate of DEZn was 1 μmol/min. Compared to the results in Fig. 2, the selective growth of ZnO nanodots was realized in this growth condition without the depletion region. Further, the average size of the ZnO nanodots is enlarged and the size uniformity deteriorates with increasing the growth temperature. The average diameters, estimated by the FE–SEM results, of the ZnO nanodots grown at different growth temperature are about 12 nm (500 °C), 13 nm (550 °C), 17 nm (600 °C), and 22 nm (650 °C).

As can be seen in the insets of Figs. 3(a) and 3(b), many ZnO nanodots were concentrated on the center of the nanopatterned lines. This fact can be explained by the shortened surface diffusion length of adatoms during the growth, which occurred due to a large number of surface atomic steps and kinks produced at the bottom of nanopatterned lines by the implantation of Ga^+ ions in accordance with the result of InAs on FIB-patterned GaAs substrates.[15] However, the increment of growth temperature usually makes the surface diffusion length of Zn adatoms longer. This fact means that the adatoms can easily diffuse with jumping over the surface atomic steps and kinks, resulting in the enlargement of dot formation areas in the nanopatterned lines as shown in the insets of Figs. 3(c) and 3(d). The inset of Fig. 3(d) shows that ZnO grown at 650 °C has a dot- and layer-mixed structure, which is attributed to the enhancement of a two-dimensional growth mode at relatively high growth temperature.

CL spectra, recorded at RT, of selectively grown ZnO nanodots at 550 and 650 °C on nanopatterned lines are shown in Fig. 4. The CL spectra are from four nanopatterned lines presented in the SEM images of Figs. 3(b) and 3(d) and consist of a broad emission band around 3.34 eV with an additional emission at about 2.7 eV. We could confirm the presence of sufficient Zn atoms from the nanodots selectively grown on FIB-nanopatterned areas by energy-dispersive x-ray analysis. This result indicates that the emission band around 3.34 eV coincides with the free exciton emission from ZnO (EX_{ZnO}) because free exciton emission becomes dominant at RT due to the ionization of impurities bounding exciton at low temperatures.[16] The EX_{ZnO} band of around 3.34 eV from the selectively grown ZnO nanodots in CL measurements is a little bit higher than that from a ZnO thin film on SiO_2/Si measured by RT photoluminescence. This result is attributed to a blue shift of the emission by a band filling effect which were originated by high energy CL excitation of 20 keV. Regarding the broad emission band located at about 2.7 eV, we speculate that it comes from defects[17] or naturally formed Si nanocrystals[18] in SiO_2 during thermal oxidation, since the same emission band is omnipresent in our SiO_2/Si substrates by CL measurements.

In summary, we have accomplished the selective formation of ZnO nanodots by MOCVD on FIB-nanopatterned SiO_2/Si substrates. The FE–SEM measurements clearly showed the selective formation of ZnO nanodots on the nanopatterned Si surface areas. The mechanism of the selective formation of ZnO nanodots on FIB-nanopatterned lines is mainly attributed to the fact that nanoscale patterns of Si act as efficient artificial traps for diffusing Zn adatoms on the surface of SiO_2 during the MOCVD growth. CL measurements recorded at RT confirmed that the emission originated from the selectively grown ZnO nanodots.

This work was partly supported by Grants for Regional Science and Technology Promotion from the Ministry of Education, Culture, Sports, Science, and Technology. One of the authors (S.-W.K.) appreciates financial support from ''International Communications Foundation (ICF), Fellowship for Researchers and Graduate Students from Abroad'' and ''The 21st Century COE Program, Project No. 14213201.''

[1] Y. Arakawa and H. Sakaki, Appl. Phys. Lett. **40**, 939 (1982).
[2] L. T. Canham, Appl. Phys. Lett. **57**, 1046 (1990).
[3] J. D. Holmes, K. P. Johnston, R. C. Doty, and B. A. Korgel, Science **287**, 1471 (2000).
[4] Y. Miyamoto, Y. Miyake, M. Asada, and Y. Suematsu, IEEE J. Quantum Electron. **25**, 2001 (1989).
[5] K. Hummer, Phys. Status Solidi B **56**, 249 (1973).
[6] M. H. Huang, S. Mao, H. Feick, H. Yan, Y. Wu, H. Kind, E. Weber, R. Russo, and P. Yang, Science **292**, 1897 (2001).
[7] S.-W. Kim, Sz. Fujita, and Sg. Fujita, Appl. Phys. Lett. **81**, 5036 (2002).
[8] T. Ishitani, A. Shimase, and H. Tamura, Appl. Phys. Lett. **39**, 627 (1981).
[9] H. J. Lexec, J. Ahopelto, A. Usui, and Y. Ochiai, Jpn. J. Appl. Phys., Part 1 **32**, 6251 (1993).
[10] S.-W. Kim, Sz. Fujita, and Sg. Fujita, Jpn. J. Appl. Phys., Part 2 **41**, L543 (2002).
[11] S.-W. Kim, Sz. Fujita, and Sg. Fujita, Mater. Res. Soc. Symp. Proc. **739**, H4.8 (2002).
[12] M. Shibata, S. S. Stoyanov, and M. Ichikawa, Phys. Rev. B **59**, 10289 (1999).
[13] B. H. Choi, C. M. Park, S.-H. Song, M. H. Son, S. W. Hwang, D. Ahn, and E. K. Kim, Appl. Phys. Lett. **78**, 1403 (2001).
[14] Y. T. Sun, E. R. Messmer, S. Lourdudoss, J. Ahopelto, S. Rennon, J. P. Reithmaier, and A. Forchel, Appl. Phys. Lett. **79**, 1885 (2001).
[15] Y. Morishita, M. Ishiguro, S. Miura, and Y. Enmei, J. Cryst. Growth **237/239**, 1291 (2002).
[16] K. Ogata, T. Kawanishi, K. Maejima, K. Sakurai, Sz. Fujita, and Sg. Fujita, Jpn. J. Appl. Phys., Part 2 **40**, L657 (2001).
[17] R. Tohmon, Y. Shimogaichi, H. Mizuno, Y. Ohki, K. Nagasawa, and Y. Hama, Phys. Rev. Lett. **62**, 1388 (1989).
[18] H. Tamura, M. Ruckschloss, T. Wirschem, and S. Veprek, Appl. Phys. Lett. **65**, 1537 (1994).